

LARGE AREA AND SCREEN PRINTED N-TYPE SILICON SOLAR CELLS WITH EFFICIENCY EXCEEDING 18%.

V.D. Mihaiilechi¹, G. Coletti¹, Y. Komatsu¹, L.J. Geerligs¹, R. Kvande², L. Arnberg², K. Wambach³, C. Knopf³, R. Kopecek⁴, A. W. Weeber¹.

¹ECN Solar Energy; PO Box 1, 1755 ZG Petten, The Netherlands.

Phone: +31 224 564113; Fax: +31 224 568214; Email: weeber@ecn.nl

²Norwegian University of Science and Technology, Faculty of Sciences, Trondheim, Norway.

³Deutsche Solar AG, Alfred-Lange Str. 18, D-09599 Freiberg/Sachsen, Germany.

⁴International Solar Energy Research Center - ISC - Konstanz, Rudolf-Diesel-Str. 15, D-78467 Konstanz, Germany.

ABSTRACT: There is currently much interest in n-type base solar cells because of potential advantages, both of silicon base material and of cell process, for high efficiency. We present results of n-base solar cells on large area multicrystalline and monocrystalline silicon wafers, produced using simultaneous diffusion of phosphorus back surface field and boron emitter, screen-printed metallization and firing through. The cell process leads to record high efficiencies of 16.4% on multicrystalline and 18.3% on monocrystalline wafers. It is experimentally demonstrated that in multi-crystalline Si a low resistivity is correlated to reduced cell efficiency, with the optimum base resistivity lying between 1.5 and 4 Ωcm . By characterizing and modeling cells from monocrystalline Si, from nominally clean multicrystalline Si, as well as from intentionally Fe-contaminated multicrystalline Si, the impact of purity on emitter recombination is investigated in more detail. Keywords: Boron, n-type, Silicon Solar Cell.

1 INTRODUCTION

n-type silicon has been proven to have a higher tolerance to common transition metal impurities, such as those present in silicon produced from quartz and carbon (via metallurgical routes), potentially resulting in higher minority carrier diffusion lengths compared to p-type substrates [1,2]. In spite of these advantages, at present, more than 85% of the silicon solar cells produced by the industry are based on p-type substrates. This is caused mostly by an insufficient development and industry implementation of the n-type cell processes for multicrystalline substrates.

This paper presents a solar cell process and cell results on n-type multicrystalline and monocrystalline wafers. The cell process is based on boron front emitter, and low cost fabrication processes for industrial use (such as screen printing and microwave plasma enhanced chemical vapor deposition (PECVD) of silicon nitride (SiN_x)). Moreover, in our experiments, in multicrystalline Si a low resistivity is correlated to reduced cell efficiency, with the optimum base resistivity lying between 1.5 to 4 Ωcm . By characterizing and modeling cells from monocrystalline Si, nominally clean multicrystalline Si, as well as intentionally Fe-contaminated multicrystalline Si, also the impact of the wafer purity on emitter properties is investigated.

2 EXPERIMENTAL DESIGN

At present, with the exception of two particular high-efficiency cell types [3,4], all silicon solar cells produced by the industry are based on p-type substrates. A substantial effort has been made in our laboratory to develop a cell process on n-type substrates which uses similar industrial techniques and processes with no substantial increase in costs. Our cell process is developed on 155.72 cm^2 phosphorous-doped n-type monocrystalline Czochralski (Cz) Si wafers with base resistivity ranging between 1 and 3 Ωcm , but results on

156.25 cm^2 industrial n-type multicrystalline Si wafers are also presented in this paper. The process begins with a texture etch (either by random pyramids or isotexture) in a chemical solution on both sides of the wafers. Subsequently, a p^+ emitter with a sheet resistance of 60 Ω/square was diffused on the front side (light receiving side) of the substrates from a boron tribromide (BBr_3) source in a quartz tube furnace of an industry-compatible scale.

As compared with industrial standard p-type solar cells, that use an aluminum alloyed rear side as a back surface field (BSF), the solar cells based on n-type substrates must have a n^+ (phosphorous) diffusion for BSF, in order to facilitate the formation of an Ohmic contact for the base metallization. In our process, phosphorous BSF has a sheet resistance of 30 Ω/square . After the diffusion processes all wafers received a standard cleaning followed by etching with a diluted hydrofluoric acid (HF) immediately before the application of the passivating layers. The passivation method used here for the front (boron emitter) and rear side (phosphorous BSF) consists of a stack of an ultrathin SiO_2 layer formed by nitric acid oxidation of Si (NAOS) [5,6] and a hydrogenated silicon nitride (SiN_x)

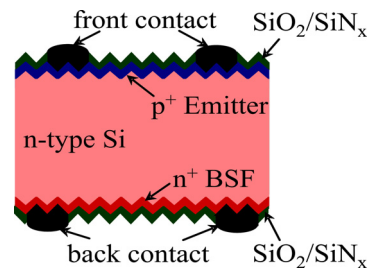


Figure 1: Schematic cross-section of the fabricated solar cells

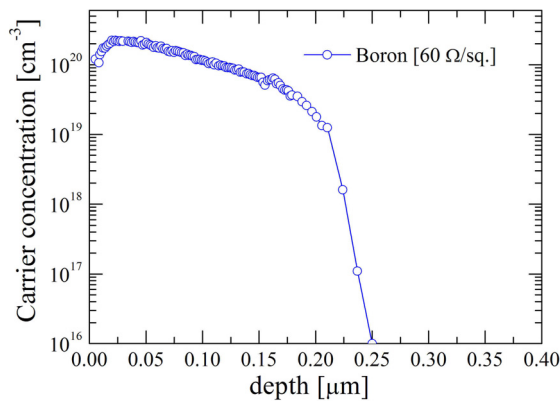


Figure 2: Carrier concentration profile for boron (emitter) diffusion measured by ECV method on a polished Cz Si wafer.

antireflection coating layer deposited by PECVD [7]. The cell process is completed with screen printing of the front and back contacts followed by a co-firing step in order to be able to make Ohmic contact between printed metal contacts and Si. A schematic layout of the fabricated solar cells is shown in Figure 1.

Figure 2 shows the resulting boron (emitter) doping profile measured on a polished Cz n-type test wafer, using the Electrochemical Capacitance-Voltage (ECV) method at ISC in Konstanz. The ECV measurements reveal a doping profile of boron emitter up to 0.25 μm depth with a visible surface depletion region. This depletion is caused by the in-situ oxidation performed to remove the boron rich layer. Further optimization seems to be needed in order to avoid this depletion region, which could enhance surface recombination of the minority charge carriers in the p^+ emitter because of an unfavorable electric field direction.

3 RESULTS AND DISCUSSION

3.1 Mono- and multi-crystalline cell results

Table I shows the best solar cell parameters, obtained using the process described above, on multi- and mono-crystalline silicon wafers. These measurements were carried out under the standard test conditions using a class A solar simulator. As can be seen from the table, a conversion efficiency of 16.4% is achieved on multi-crystalline n-type substrates and nearly 1% absolute higher efficiency on monocrystalline Cz substrate. With the difference coming from short-circuit current (J_{sc}) and open-circuit voltage (V_{oc}) it suggests that bulk lifetime may still be an important limitation for multicrystalline n-type cells. A more quantitative analysis will follow later in this paper.

Nevertheless both, mono- and multicrystalline, cell efficiencies of table I represent the highest values reported for an n-type industrial process using screen-printed and fired-through metallization on large area substrates (exceptions are the high-efficiency cell concepts of Sunpower and Sanyo [3,4]). This represents a significant step forward for industrial production of solar cells based on n-type substrates. Moreover, further improvements are expected (especially in the fill factor)

Table I: Comparison of the best solar cell parameters measured under standard test conditions (AM1.5G, 100 mW/cm^2 , 25 $^{\circ}\text{C}$). The solar cells were fabricated on 156.25 cm^2 multicrystalline Si substrates and 155.72 cm^2 monocrystalline Cz Si. The average efficiency of the 10 monocrystalline cells with random pyramids texture etch was 17.9%. The base resistivity is 1.8 Ωcm for the multicrystalline cells and 1.5 Ωcm for the Cz cells.

Wafer	Surface texture	J_{sc} [mA/cm^2]	V_{oc} [mV]	FF [%]	η [%]
mc-Si	isotexture	35.2	607	76.7	16.4
Cz	isotexture	36.3	629	75.8	17.3
Cz	r.pyramids	37.3	630	77.8	18.3

for solar cells processed on isotexture etched surface. We have explored the benefits of this n-type process over the more developed and widely applied p-type process, and work is underway to industrialize the n-type process.

3.2 Effect of base resistivity

In the following we have investigated solar cells fabricated on wafers belonging to different n-type multicrystalline Si ingots with difference in their base resistivity, with the purpose to find out the optimum resistivity range for n-type multi-crystalline Si ingots and cells. Two multicrystalline n-type ingots grown in the same furnace have been selected for this investigation: a compensated ingot (called ingot 5) which is partially p-type (boron) and partially n-type (antimony) doped. Such a compensated ingot is very well suited for this type of investigation as it allows for a large variation in wafer resistivity on a narrow part of the ingot size, while variation in concentration of metal impurities and crystal defects is relatively small. The other n-type ingot (called ingot 6 /antimony doped) that we have investigated has resistivity ranging from 2.2 to 0.3 Ωcm from bottom to top of the ingot. Solar cells have been fabricated (using the process described above) on 156.25 cm^2 wafers distributed to cover a resistivity range of 0.8 to 7.7 Ωcm from ingot 5 and 0.3 to 2.2 Ωcm from ingot 6.

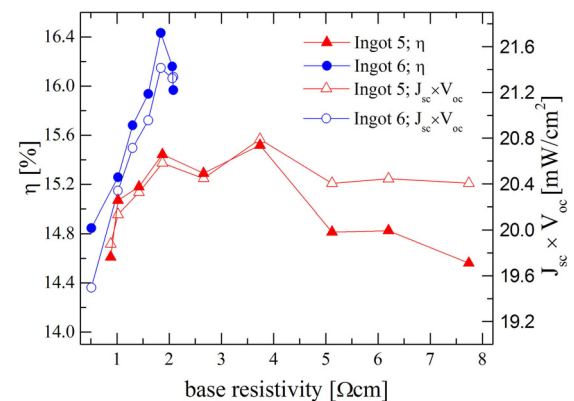


Figure 3: Experimental power conversion efficiency η and $J_{\text{sc}} \times V_{\text{oc}}$ product versus base resistivity of both multicrystalline n-type Si ingots investigated.

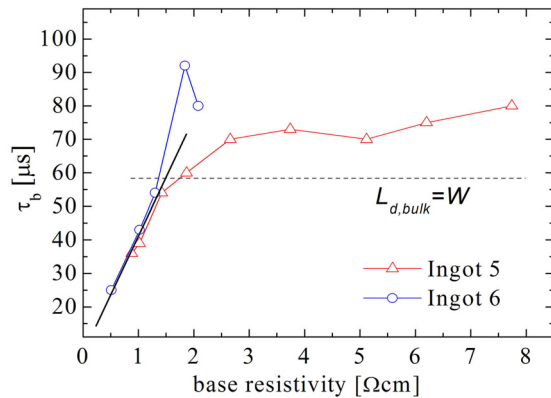


Figure 4: Minority carrier lifetime in the bulk τ_b determined from the PC1D fit of IQE data as a function of wafer base resistivity.

Figure 3 shows the experimental conversion efficiencies (η) and $J_{sc} \times V_{OC}$ product as a function of base resistivity for both ingots investigated. As seen from the figure the best results are obtained for wafers belonging to ingot 6, with the highest performance obtained around 25% from the bottom of the ingot. The parameters of the best cell measured are shown in table I. Another interesting result that can be observed in figure 3 is that the $J_{sc} \times V_{OC}$ product continues to rise for cells made from ingot 6 as resistivity is increased while it stays rather constant for cells of ingot 5 for resistivities larger than 1.3 Ωcm . Above 3.5 Ωcm a decrease in η of ingot 5 is, however, caused by a decrease in FF. This decrease in FF is a result of a higher series resistance. Nevertheless, we show that the optimum base resistivity for n-type multicrystalline Si feedstock lies between 1.5 to 4 Ωcm (these values can be lower if thinner wafers are produced) in order to maximize the efficiency output throughout the ingot.

Figure 4 shows the bulk lifetime (τ_b) resulting from fitting the internal quantum efficiencies (IQE) data of the cells from both ingots investigated. From lifetime data it is observed that a resistivity higher than approximately 1.3 Ωcm is required in order to ensure that bulk diffusion length $L_{d,bulk} > W$ (W is the averaged wafer thickness of all investigated cells) for both ingots. For $L_{d,bulk} < W$, that means a resistivity $< 1.3 \Omega\text{cm}$, both ingots have almost identical lifetime even though this threshold occurs for wafers of $>50\%$ towards the top of the ingot 6 and only $>85\%$ towards the top of ingot 5. Notably, the lifetime as a function of resistivity shows for low resistivity a linear dependence, suggesting activity of some impurity which is relatively harmful in n-type base (e. g. Au, Zn, perhaps Cr) [1,8,9].

3.3 Effect of impurities on emitter recombination

While the n-type base of the solar cells may be expected to be less sensitive to many transition metal impurities, the p^+ emitter could rather be more sensitive. It is commonly believed that recombination into the highly doped emitter region is dominated by Auger and radiative recombination. Recent investigations, however, show that relatively large amounts of metal impurities (e.g., Fe, Cu, Cr) can be getterd in a n^+ (phosphorous) emitter during

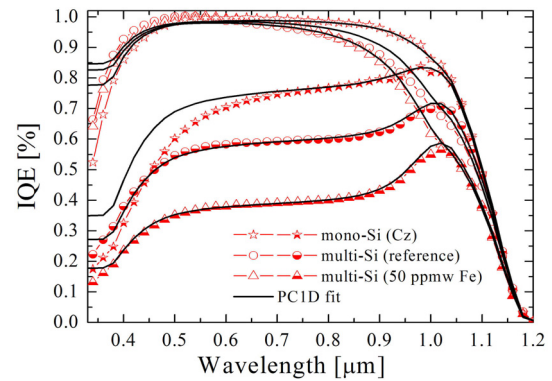


Figure 5: Front (empty symbols) and rear side (semi-filled symbols) IQE of solar cells fabricated from a mono-crystalline (Cz) ingot, a reference multi-crystalline, and a multi-crystalline ingot with 50 ppmw of Fe. The solid lines represent the PC1D calculation considering the emitter recombination parameters from table II.

diffusion processes [10]. These getterd impurities have relatively low impact on a n^+ emitters due to their higher capture cross-section of electrons as compared with holes.

In order to verify that metal contamination of the p^+ emitters can indeed have a significant effect, n-type solar cells were fabricated (using the process described in this paper) from clean monocrystalline (Cz) wafers, nominally clean multicrystalline Si wafers, and multicrystalline Si wafers from feedstock intentionally contaminated with 50 ppmw of Fe [11]. The resulting IQE and I-V data were modeled using PC1D simulation program taking into account measured front and rear doping profiles, surface reflection, base resistivity, and wafer thickness. The relevant fit parameters left for the modeling are τ_b , front and rear surface recombination velocities (SRV), and emitter recombination. The latter parameter has been introduced in our PC1D model as a separate emitter region with an effective diffusion length ($L_{d,emitter}$) taken at an acceptor density of $N_A = 10^{20} \text{cm}^{-3}$. By fitting both front and rear IQE data all fit parameters can readily be determined. The results show that only τ_b (or $L_{d,bulk}$) and $L_{d,emitter}$ needs to be varied between various cells with a constant front SRV of $1.0(\pm 0.5) \times 10^4$ cm/s (on boron emitter) and rear SRV of $1.0(\pm 1) \times 10^5$ cm/s (on phosphorous BSF). A constant SRV is expected since all solar cells have been processed in the same run.

Figure 5 shows the experimental IQE curves (symbols) of selected cells from the three different ingots together with the PC1D fit using the model discussed above. The front IQE clearly does not indicate a variation in front surface passivation. However, without including recombination active defects in the emitter ($L_{d,emitter} \gg W_{emitter}$), the PC1D calculated V_{OC} and the experimental V_{OC} of the cells deviate significantly. The deviation varies from 6 mV for the Cz wafer, to 22 mV for the Fe-contaminated wafer. This deviation can be fitted well (without affecting the IQE curves) by including interstitial Fe defects into the p^+ emitter. Of course, interstitial Fe is a likely contaminant that can affect the diffusion length in the emitter, but also other

Table II: PC1D fit parameters used in figure 5. $L_{d,emitter}$ is taken at $N_A = 10^{20} \text{ cm}^{-3}$, whereas ΔV_{OC} represents the difference between calculated V_{OC} , when only Auger recombination is considered in the emitter, and measured V_{OC} of the cells.

Wafer	$L_{d,bulk}$ [μm]	$L_{d,emitter}$ [μm]	equiv. Fe_i [cm^{-3}]	ΔV_{OC} [mV]
Cz	841	0.56	9×10^{14}	6
mc-Si (reference)	284	0.47	2×10^{15}	14
mc-Si (50 ppmw Fe)	192	0.41	4×10^{15}	22

impurities may be present. Thus, the interstitial Fe concentration is used here as a convenient parameter to represent increased Shockly-Read-Hall emitter recombination in general. The resulting fit parameters are shown in table II. It was found that consideration of this contamination was essential to simultaneously fit IQE curves as well as V_{OC} correctly. Incidentally, it can be seen that the 50 ppmw of Fe have only modest effect on $L_{d,bulk}$ of the solar cells but it can bring significant limitation to V_{OC} due to the emitter contamination. Further analysis of this effect is in progress.

Based on fitted IQE of different multicrystalline and monocrystalline cells and using our model calculation we were able to identify the efficiency enhancement possibility for our n-type cell process. Figure 6 shows the experimental efficiencies of the cells of figure 5. These efficiencies are plotted together with the calculated curve against the ratio of minority carrier diffusion length in the bulk and wafer thickness ($L_{d,bulk}/W$), assuming an isotexture etched surface, same metallization shadowing, FF, and W, for all cells. A good agreement is observed for all cells allowing us to quantify the relation between material quality (given by $L_{d,bulk}$) and the resulting solar cell efficiency when all other parameters of the process are the same. Work is underway to elucidate the relation between $L_{d,bulk}$ and the presence of some defects in mc-Si wafers [11].

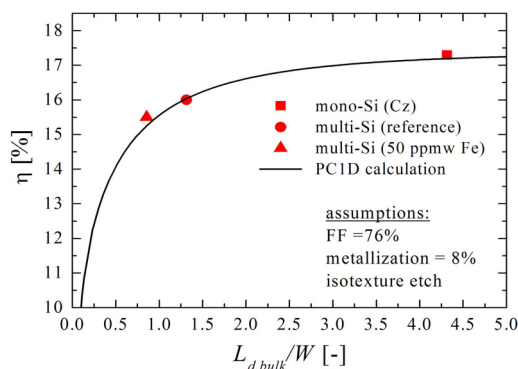


Figure 6: Calculated (solid line) and experimental (symbols) efficiency as a function of minority carrier diffusion length and wafer thickness ratio ($L_{d,bulk}/W$).

4 CONCLUSION

We have demonstrated a process to fabricate n-type solar cells on large area (156.25 cm^2) multicrystalline and mono-crystalline Cz substrates, involving diffusion of phosphorus BSF and boron emitter, screen-printed metallization and firing through, leading to efficiencies of 16.4% on multicrystalline Si and 18.3% on Cz. Experiments on wafers of different base resistivity show that the optimum target resistivity for n-type multicrystalline silicon wafers lies between 1.5 to 4 Ωcm in order to maximize the efficiency output thorough the ingot. In multicrystalline cells, modeling gives a clear indication that contaminants inside the wafer affect the emitter recombination.

ACKNOWLEDGEMENTS

This work was supported by the European Commission within the FoXy project under the contract number 019811(SES6), and by the Dutch agency for energy and the environment SenterNovem. ECN acknowledges cooperation with Tempres.

REFERENCES

- [1] D. MacDonald, L. J. Geerligs, Appl. Phys. Lett. 85, 4061 (2004).
- [2] J. E. Cotter et. al., 15th Workshop on Crystalline Silicon Solar Cells & Modules: Materials and Processes, p. 3 (2005).
- [3] M. Taguchi, A. Terakawa, E. Maruyama, M. Tanaka, Progr. Photovolt. 13, 481 (2005)
- [4] K. R. McIntosh, Proc. of the 3rd World Conf. on Photovoltaic Energy Conversion, p. 971 (2003).
- [5] Asuha, S. Imai, M. Takahashi, H. Kobayashi, Appl. Phys. Lett. 85, 3783 (2004).
- [6] Asuha, Y. Liu, O. Maida, M. Takahashi, H. Kobayashi, J. Electrochem. Soc. 151, 824 (2004).
- [7] V. D. Mihaletchi, Y. Komatsu, L. J. Geerligs, Appl. Phys. Lett. 92, 063510 (2008).
- [8] L. J. Geerligs and D. H. Macdonald, Progr. Photovolt. 12, 309 (2004).
- [9] J. Schmidt et al., Proc. of the 22nd European Photovoltaic Solar Energy Conf., p. 998 (2007).
- [10] A. Bentzen, A. Holt, R. Kopecek, G. Stokkan, J. S. Christensen, B. G. Svensson, J. Appl. Phys. 99, 093509 (2006).
- [11] G. Coletti, R. Kvande, V. D. Mihaletchi, L. J. Geerligs, L. Arnberg, E. J. Øvrelid, J. Appl. Phys. (to be published).